

Simulation study of a two stream instability with a beam $\gamma = 100$

M.E. Dieckmann¹, P.K. Shukla¹, L.O.C. Drury²

¹ *Theoretische Physik IV, Ruhr-Universität Bochum, D-44780 Bochum, Germany*

² *Dublin Institute for Advanced Studies, 5 Merrion Square, Dublin 2, Ireland*

Abstract

A better understanding of the relaxation of relativistic plasma flow is required to identify particle acceleration and radiation generation mechanisms at gamma ray bursts (GRBs). We perform particle-in-cell (PIC) simulations of the electrostatic two-stream instability for a beam speed v_b with $\Gamma(v_b) = 100$. The two p^+e^- beams are charge neutral and have comparable densities. The instability saturates by trapping the electrons of one beam and it modulates the electron density of the second beam. The electrostatic fields are compressed in the forming cavities to high intensities. The waves collapse, after which the electrons show an exponential tail that is eventually transformed into a power law tail.

Introduction

Jets are found in systems of accreting black holes that range from microquasars through active galactic nuclei to some gamma ray bursts (GRBs). GRB jets can have Lorentz factors of $10^2 < \Gamma < 10^3$ and the low collision frequency of the ambient plasma particles implies that they relax by collisionless mechanisms. The internal/external shock model [1] assumes the formation of an external shock between the jet plasma and the ambient plasma. The collision of plasma components within the jet, which move at different speeds, is leading to internal shocks. Typically, the plasma thermalisation at the internal shock is associated with the prompt emissions of a GRB, whereas the external shock is associated with the afterglow [1].

The jet front is sketched in Fig. 1. The formation of an ultrarelativistic external shock has been questioned, since ultrarelativistic plasma flows are more unstable to the filamentation instability [2] than to two-stream instabilities. Only the latter probably give rise to planar shock

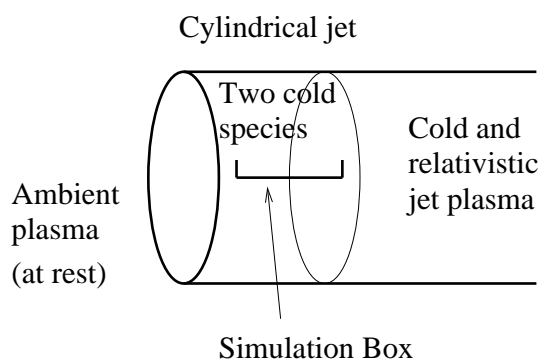


Figure 1: A relativistic jet is expanding into the ambient plasma. The jet plasma and the upstream plasma overlap and the thermalisation processes take place in this spatial interval.

fronts. PIC simulations [3] are thus employed to examine the plasma thermalisation.

The simulation

The importance of the Weibel instability [4] for the magnetic field generation at the colliding plasmas has been demonstrated [5, 6]. The electron heating in [5, 6] can, however, probably not be attributed to the purely electromagnetic Weibel mode. The mixed modes [7] may be involved, because their electrostatic component can heat electrons. We demonstrate a consequence [8, 9] of such an electrostatic component in ultrarelativistic flows: **Cavitation** [10].

PIC simulations solve the Maxwell's equations and the relativistic Lorentz equation for many computational particles, each with index i . The particles and the fields are connected through the current \mathbf{j} .

$$\nabla \times \mathbf{B} = \mu_0 \mathbf{j} + \epsilon_0 \mu_0 \frac{\partial \mathbf{E}}{\partial t}, \quad (1)$$

$$\nabla \times \mathbf{E} = -\frac{\partial \mathbf{B}}{\partial t}, \quad (2)$$

$$\frac{d\mathbf{p}_i}{dt} = q(\mathbf{E} + \mathbf{v}_i \times \mathbf{B}). \quad (3)$$

We place a one-dimensional periodic simulation box in the overlap region of the jet and the ambient plasma (Fig. 1). Initially, two interpenetrating and spatially homogeneous beams of electrons and protons are placed in the simulation box. The background plasma is at rest and the beam moves with the speed v_b , resulting in $\Gamma(v_b) = (1 - v_b^2/c^2)^{-1/2} = 100$.

All plasma components have the temperature 400 eV. The beam velocity is aligned with the x -direction and $\mathbf{B} = 0$. \Rightarrow Only the x, p_x components are involved during the electrostatic instability. The density ratio between the background plasma (n_p) and the beam plasma (n_b),

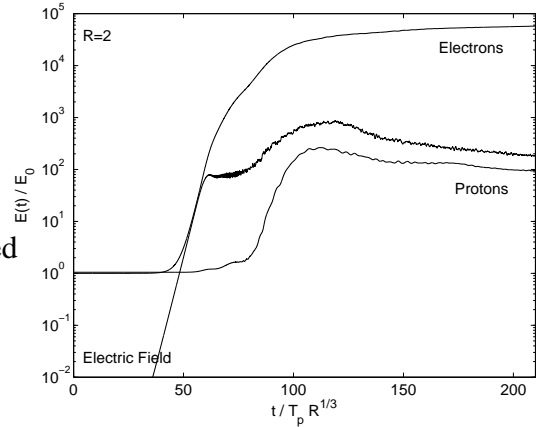


Figure 2: The energy densities, normalized to the initial electron thermal energy density E_0 , of the electrostatic field, the background electrons and protons.

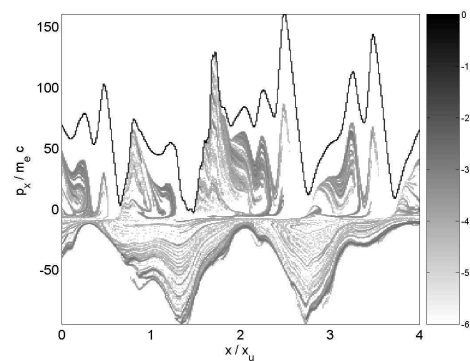


Figure 3: The electron phase space distribution at $t \approx 100 T_p R^{1/3}$. The background electrons have been scattered. The beam electrons are still cool and show momentum oscillations.

in their respective rest frames, is $R = n_p/n_b = 2$.

The electron plasma frequency and plasma period are $\omega_p = (n_p e^2 / m_e \epsilon_0)^{1/2}$ and $T_p = 2\pi / \omega_p$.

Two-stream unstable waves grow at the exponential rate $\gamma_i = \sqrt{3} / \Gamma^{2/3} (v_b) R^{1/3} 2^{4/3}$. Fig. 2 shows that the electrostatic wave saturates initially at the time $t / R^{1/3} T_p \approx 50$, by its interaction with the electrons (trapping) [9]. The initial saturation involves only electrons, which continue to accelerate after the wave saturation. Proton heating takes place at $t \approx 100 T_p R^{1/3}$ and the associated electron distribution is shown by the Fig. 3.

The initially trapped electrons of the background plasma have been scattered over a broad phase space interval. The electrostatic fields associated with their charge density modulation accelerate the beam electrons. The electric fields are compressed by the growing oscillations of the electron beam and a runaway process develops. An exponential energy tail forms for the electrons and the protons accelerate.

Energy transfer between electrons and protons is enabled by the electrostatic fields. The growing density fluctuations of the proton beams may imply stochastic wave-particle interactions \Rightarrow Power law distribution (Fig. 5). This slope matches that reported by [6] and the electrostatic fields originating from the proton beam density fluctuations may be responsible for the final plasma thermalisation also in 3D PIC simulations.

Summary

* An electrostatic component of a streaming instability may yield cavitation effects due to the modulation of the cool electron beam by the strong electrostatic fields associated with the scattered and hot background electrons.

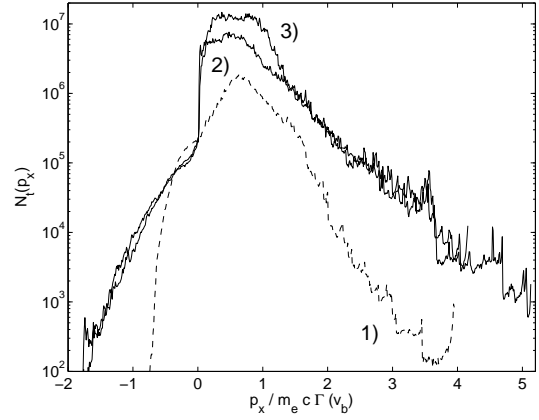


Figure 4: The electron distributions at the time $t / T_p R^{1/3} = 120$ in simulations with $R = 10$ (curve 1), $R = 2$ (curve 2) and $R = 1$ (curve 3). The electron high energy tails are exponential for $R = 1, 2$ and it is approaching an exponential for $R = 10$.

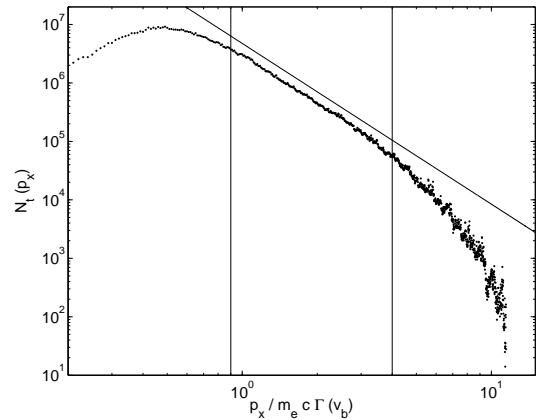


Figure 5: The electron momentum distribution for $R = 2$ at $t / R^{1/3} T_p = 208$. Over a limited momentum interval, it decreases as $N(p_x) \sim p_x^{-2.7}$.

* Cavitation can accelerate electrons to energies comparable to 10 times the jet speed for the plasma parameters considered here. This acceleration is robust, provided both beams have densities that agree to within a factor of 10.

* \Rightarrow Electron acceleration may be possible even if no streaming instability develops, e.g. if a hot (noisy) jet encounters a cold upstream plasma.

* The strong electrostatic fields can modulate the proton beams and their charge density fluctuations can randomize the electrons \Rightarrow power law energy distribution.

Acknowledgements

The DFG and the Dublin Institute for Advanced Studies (DIAS) have financially supported this work. The Swedish NSC and Irish ICHEC have provided the computing resources.

References

- [1] T. Piran, Rev. Mod. Phys. **76**, 1143 (2004)
- [2] J.J. Brainerd, Astrophys. J. **538**, 628 (2000)
- [3] J.W. Eastwood, Comput. Phys. Commun. **64**, 252 (1991)
- [4] E.S. Weibel, Phys. Rev. Lett. **2**, 83 (1959)
- [5] L.O. Silva, R.A. Fonseca, J.W. Tonge, J.M. Dawson, W.B. Mori and M.V. Medvedev, Astrophys. J. **596**, L121 (2003)
- [6] C.B. Hededal and K.I. Nishikawa, Astrophys. J. **623**, L89 (2005)
- [7] A. Bret, M.C. Firpo and C. Deutsch, Phys. Rev. Lett. **94**, 115002 (2005)
- [8] M.E. Dieckmann, P.K. Shukla and L.O.C Drury, MNRAS **367**, 1072 (2006)
- [9] M.E. Dieckmann, Phys. Rev. Lett. **94**, 155001 (2005)
- [10] V.E. Zakharov, Zh. Eksp. Teor. Fiz. **62**, 1745 (1972)